Experimental study of a confined premixed metal combustor: Metal flame stabilization dynamics and nitrogen oxides production

Driss Laraqui, Olivier Allgaier, Cornelius Schonnenbeck, Gontrand Leyssens, Jean-Francois Brilhac, Ricardo Lomba, Clément Dumand, Olivier Guézet

Experimental study of a confined premixed metal combustor:

metal flame stabilization dynamics and nitrogen oxides production.

Driss Laraqui[1,2], Olivier Allgaier[1], Cornelius Schönnenbeck[1], Gontrand Leyssens[1], Jean-François Brilhac[1], Ricardo Lomba[3], Clément Dumand[2], Olivier Guézet[2]*

[1]*Université de Haute-Alsace, LGRE-EA2334, Mulhouse, France*

[2]*Groupe PSA, Centre Technique de Vélizy, Route de Gisy, 78943 Vélizy Villacoublay Cedex, France*

[3]*AVL LMM SAS, 5-9 rue Benoît Frachon, F-91127, Palaiseau-Cedex, France*

**Corresponding author:*

Pr. Jean-François Brilhac

Mailing address: Laboratoire Gestion des Risques et Environnement (EA2334), Université de Haute-Alsace, 3bis rue Alfred Werner, 68093 Mulhouse Cedex, France

E-mail: jean-francois.brilhac@uha.fr

Colloquium: Solid Fuel Combustion

Total paper length (Method 1): 6053

Main text: 4471; equations: 68.4; references: 506.92; figure 1 and caption: 213.92; figure 2 and caption: 115.12; figure 3 and caption: 134.18; figure 4 and caption: 136.18; figure 5 and caption: 136.18; figure 6 and caption: 133.18; figure 7 and caption: 138.18

Authors affirm to pay color reproduction charges if applicable.

Abstract

This work presents a study of a magnesium/air combustion process in the context of innovative zero carbon dioxide (CO_2) energy carriers for reducing global warming effects. In order to analyze more deeply the confined combustion of magnesium under fluctuating overpressure conditions (0 to 24hPa) and the generated gaseous by-products, magnesium/air flames have been realized in a combustion chamber with a conical bluff-body as flame holder and different contraction ratios diaphragms at the exit duct. Sieved magnesium samples with two size-fractions were tested: 20-50 µm and 50-70 µm. The gaseous emissions of nitrogen oxides (NO_x) and dioxygen (O_2) were analyzed with on-line infrared, ultraviolet and paramagnetic analyzers. A flame pulsating behavior was clearly observed from light emission intensity (monitored by a photodiode) and pressure fluctuations (monitored by a pressure sensor); the frequencies obtained ranged between 3 to 10 Hz. The frequency of the pulsation exhibited strong dependence on the geometric configuration of the chamber: a contraction diaphragm divided by two the frequency level of the fluctuations in the studied range of maximum overpressure. Such fluctuations may probably be the consequence of periodic perturbations of the recirculation zone behind the bluff-body. These periodic perturbations are themselves caused by strong periodic overpressure variations due to stiff contraction downstream responding to gas velocity fluctuations. This feed-back-loop mechanism was considered in this study. NO_x emissions produced through the thermal pathway were analyzed for equivalence ratios ranging from 0.29 to 1. The representation of NO_x versus equivalence ratio exhibited a parabolic shape with a maximum for an equivalence ratio of 0.4. Moreover, NO_x emissions of this metal combustor have shown a similar order of magnitude than current internal combustion engines.

Keywords: Metal combustion; Combustion instabilities; Bluff-body stabilized flames; NO_x emissions ; Clean energy sources

1. Introduction

In a context of global warming and fossil fuel scarcity, finding a zero greenhouse gases power source is a concern in every field of human activity. Metal particle combustion has been investigated since the 1960s,

for military, mining or space propulsion purposes for instance as supplementary heat source in solid rocket boosters [1]–[3]. More recently, metal particle combustion has been seen as a potential alternative energy source for transportation or stationary applications [4], [5]. The possibility of capturing and recycling metals oxides is the cornerstone of this innovative energy pathway, in which metals could be considered a quasi-renewable energy carrier [6]. In the available literature, magnesium has been compared to other metals and is a relevant candidate due to its less complex chemistry and its burning properties. Magnesium (Mg) combustion produces only magnesium oxide (MgO) and has a higher burning rate than other metals due to its relatively high volatility [7]. Moreover, magnesium is sufficiently abundant on the earth crust for cycle initiation and is largely underused in comparison to aluminum and iron. For instance, iron is four times more present in the earth's lithosphere than magnesium but it was four thousand times more used in 2011 [8]. Nevertheless, many challenges arise when considering magnesium or any other metal as a future fuel for high power demanding applications. From a combustion aspect, one of the challenges is to achieve high volumetric heat release rates in a confined volume under high-pressure drop conditions induced by filtration or gas after-treatment systems. Bluff-body flame stabilization and many others means of stabilization in such high velocity flow conditions have already been widely studied [9]–[11]. Generated combustion instabilities in unsteady flame stabilization context, caused, for instance, by vortex shedding interaction with acoustic modes, are an issue which occurs in confined fast streams combustors such as those in rockets, ramjets and afterburners [12]–[14]. Simultaneous measurements of pressure and light emission intensity fluctuations are usual means used when studying combustion instabilities as their coupling to acoustic modes is characterized by the Rayleigh criterion [15] and which is mostly the source term of the instability. These previously mentioned instabilities are essentially exhibiting high frequencies. The case of lowest frequencies has been presented by Langhorne [16]: the reheat buzz ranging from 50 to 150 Hz. No study was found about confined combustion instabilities under high-pressure drop presenting lower combustion oscillations frequencies.

Considering the depollution aspect, nitrogen oxides (NO_x) are known as an environmental and health issue if they are not reduced in a sufficient way [17]. High temperature conditions, during fuel combustion with air,

are known to produce excessive thermal nitrogen oxide (NO) through a thermal pathway studied by Zeldovich et al. [18]. Consequently, studies on NO_x emission and reduction means of internal combustion engine (ICE) were extensively carried during this last decade. On the contrary, NO_x emissions from a metal flame were rarely investigated, see a first glance by Garra et al. [19]. To our knowledge, the influence of a metal-air ratio regime on NO_x emission has never been reported.

For the present study, magnesium/air flames have been realized in a combustion chamber with a conical bluff-body as flame holder and several contraction ratio diaphragms at the exit duct. The study aims to observe and analyze the flame instabilities using simultaneous pressure sensor and photodiode measurements. A feed-back-loop mechanism is deduced from the observations. The investigation of NO_x emissions has also been carried out in a wide range of equivalence ratios from 0.29 to 1.

2. Experimental setup and procedures

2.1. The combustion system

a. Metal fuel and injection description

The experiments were conducted with a polydisperse aerosol of pure magnesium powder (>99.8%) supplied by Carl Roth as CP20.2 reference. Two size fractions were prepared using a siever RETSCH AS200: 20-50µm and 50-70µm. The obtained size-distribution has been measured using a Laser granulometer Scirocco 2000 M from MALVERN and a Sauter mean diameter D_{32} was then attributed to the two-size fractions 20-50µm and 50-70µm which is respectively equal to 38 µm (±3µm) and 64 µm (±2 µm).

Solid fuel injection was performed using a PALAS BEG 1000 type B which allows to generate the aerosol of the targeted mass flow rate. The mass injection rate was monitored by a KERN FKB 16K0.05 weighting scale.

The solid fuel injector uses a Venturi system. Air flowing through a Venturi channel causes a depression which sucks powder and air from a container, generating an aerosol thanks to a fast rotating brush uplifting the powder carried on a conveyor belt. This system is widely used as it ensures continuous and homogeneous injection.

The injection system was not fully confined as supplementary air was sucked into the system with the solid. The amount of supplementary air depends on the powder mass flow rate and is calculated using the mass balance of magnesium and air through measured equivalence ratio and powder mass flow rate. Although this supplementary air was found to represent up to 20% of the initial air mass flow for very low magnesium concentration, typical values were of about 10%, and this effect is systematically accounted for in the measurements.

b. Combustor configurations

The axisymmetric combustor consists of an inlet duct, a short dump followed by a ramp, a combustion chamber with a bluff-body as a flame holder and a pressure drop regulator downstream the chamber. A scheme of the combustor is given in Fig. 1.

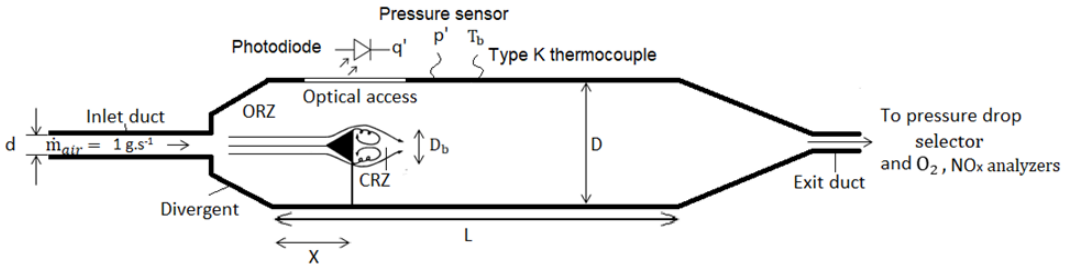

Fig. 1: Scheme of the experimental setup

The expansion ratio *D/d* is 5:1. A conical bluff-body was set at a constant distance from the divergent of about 0.75*D*, with a blockage ratio $\xi = Db/D$ of 20%. The conical shape of the flame-holder, with an apex angle of 40°, allowed the magnesium/air mixture to flow around it without any significant sticking as visually observed after each experiment. The bluff-body was supported by a stem supposed to be aerodynamically shaped and thin enough (0.03*D* width) to ensure no disturbances of the flow pattern by a separation of stream lines on its surface. Three lengths *L* were considered for the combustion chamber (4*D*, 6*D*, 10*D*) to observe the effects of such a parameter on the combustion instability and NO_x production. An optical access of 2*D* long and *D*/3 high in the cylindrical combustion chamber has been realized to visualize and measure the flame emission.

Diaphragms generating diameter contraction ratios of 14.3:1, 12.5:1, 11.1:1 were inserted between the reactor and the exhaust duct, in order to change the pressure drop level in the combustion chamber from 13 to 24 hPa. Different levels of maximum pressure drops (± 15% variability) appeared in intermittence for each diaphragm. That allowed to get a set of nine maxima of overpressure in the considered range.

c. Mean flow conditions and experimental procedure

The air mass flow was 1 $g.s^{-1}$ with small variations as previously discussed due to air suction in the solid injection system. The Reynolds number (Re = 8 x 10^3) was estimated from the inlet duct air velocity $\bar{V}_{inlet}$, bluff-body diameter D_b and kinematic viscosity at ambient air temperature T_u. A one-phase flow behavior was assumed, as the volume fraction of the metal particles in the flow for all experimental conditions is about 0.01% at most. The corresponding related inter-particle space is approximately equal to 17 and is high enough (>10) to consider the flow as highly diluted with one-way flow on particle coupling [20]. Measurements of the mean axial velocity profile were performed using a Testo 480 with a hot-ball probe, for non-reacting flow without bluff-body, which showed a turbulent profile in the flame zone. The impact on the flame stabilization of the outer recirculation zone (ORZ) presumably located near the divergent walls was assumed to be less significant than the prominent role of the recirculation zone behind the bluff-body (CRZ) in a first approximation. Experiments have indeed shown that the former could not stabilize the flame without the presence of a bluff-body.

The magnesium/air flame was ignited by an oxyacetylene torch, which was directed in a perpendicular way to the flow and located at the junction between the divergent and the combustion chamber. This location allowed a heating up of the gas inside the chamber without any direct thermal impact on the bluff-body. The torch nozzle was hidden to avoid any unintended flow disturbance. Quenching of the flame is performed by simultaneous inerting by N_2 and interruption of fuel injection.

Below stoichiometric conditions, an equivalence ratio is indirectly obtained from dioxygen (O_2) monitoring at the outflow of the combustion chamber to account for the volume flow perturbations. Admitting that almost 100% conversion of magnesium for every fuel/air ratio (minimum measured value was found to be

97%) is obtained, the following relation is used to compute the equivalence ratio (more details on gas emission analysis are given in section 2.2 hereafter).

$$\varphi = \frac{\%O_{2,initial} - \%O_{2,combustion}}{\%O_{2,initial}} \qquad (1)$$

Twelve equivalence ratios for the two Sauter mean diameters ranging from 0.29 ± 0.046 to 0.98 ± 0.03 were studied. The lowest equivalence ratio which has been reached corresponds to the lower limit of stability of the combustor.

2.2. Diagnostic tools

a. Measurement instrumentation for unsteady parameter measurements

The flame emission intensity characterizes the heat release rate from the metal combustion in the combustion chamber. Such intensity was measured using a photodiode OPT101 from Texas Instrument covered with a grey filter oriented through the optical access. Its sensitivity was further modulated using higher electric resistances (50kΩ to 1MΩ) in order to adapt signal-to-noise ratio which depends on the targeted scale. The pressure fluctuations were monitored using a pressure converter and sensor JUMO TYP 404 304 with a precision of 1hPa in the range 0-100 hPa. Data acquisition was then performed using a 2 channel 16 bit digital storage oscilloscope Mephisto scope 1 from Meilhaus. The sampling frequency was 2.5 kHz. The frequency spectra corresponding to intensity and pressure signals were obtained by Fast Fourier Transform with a resolution ranging from 0.03 Hz to 0.2Hz depending on the duration of the stabilized signal. The resolution was taken as the main experimental uncertainty of the frequencies measurements. The signal-to-noise ratio varies from 10:1 to 16:1.

A CANON EOS 1200D 50 fps camera equipped with a 499 nm filter was used to visualize the flame contours during the pulsation.

b. Measurement instrumentation for steady state characterization

The mean burnt gas temperature T_b was determined using a thermocouple located at a distance of 2D from the divergent (± 5 to 10K precision). O_2 and NO/NO_2 mole fractions in the exhaust flows were measured using paramagnetic, infrared and ultraviolet cells of X stream Rosemount analyzers and are expressed in %Vol and ppm, respectively. The gas composition, the gas temperature as well as the weighting scale signal were recorded with a frequency of 1 Hz.

In order to estimate the completion of the reaction, samples of unburnt magnesium were collected within the combustion chamber. A muffle furnace (Naberterm LT5/P330) was used to oxidize the collected Mg/MgO sample under a linear heating ramp during 3 hours up to 1123 K. The combustion completion or efficiency η was then calculated from:

$$\eta = 1 - \frac{\%massgain(sample)}{\%massgain(max)} \qquad (2)$$

Where $\%massgain(sample)$ is the mass gain of the collected sample and $\%massgain(max)$ is the maximum theoretical mass gain which can be obtained from a complete oxidation of a magnesium sample. Only the local efficiency in the cylinder around the bluff-body was studied. In other parts of the combustor, the combustion efficiency slightly varied below 100%, in comparison with the bluff-body region where it varied between 75% and 97% depending on the experimental conditions (as discussed hereafter).

3. Results and discussion

3.1. Investigation on the flame pulsating behavior

A periodic combustion was observed through the optical access as illustrated by an example of seven successive pictures of the flame in expansion in Fig. 2.a. The drawn contours tend to overestimate the flame location due to strong light diffusion and image saturation. Figure 2.b shows a scheme of what could be observed on pressure and light signals during a period of oscillation of the flame. p'_m and q'_m are the maximum overpressure and the maximum heat release rate, respectively. The combustion time $t_{combustion}$ and the combustion-pressure delay Δt are also indicated with realistic proportions. Considering the available

information, this section aims at proposing a first description of the phenomenon leading the pulsating flame behavior.

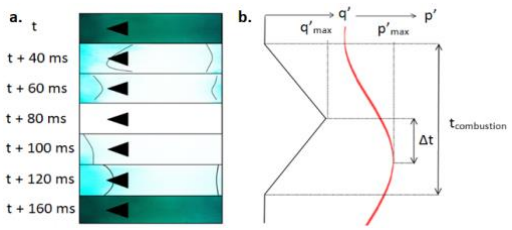

Fig. 2: a. Successive pictures of the flame expansion (the bluff-body is represented by a triangle).
b. Schematic representation of the corresponding pressure and light emission fluctuations measured.

This unsteady behavior at very low frequency level could be the consequence of different phenomena. On one hand, a vortex shedding frequency which could be generated depending on flow conditions and, on the other hand, the coupling between the flame heat release rate and the pressure fluctuations through solid injection or bluff-body wake perturbation. The possibility of an acoustically coupled combustion with the analysis of Rayleigh's criterion [15] was not investigated as the observed frequencies were two orders of magnitude lower than the combustion chamber resonant modes. Vortex shedding, periodic solid injection interruption and periodic wake destruction are considered in the following subsections and a scenario for the combustion instability mechanism is subsequently proposed.

a. On the possibility of a vortex shedding driven instability

A vortex shedding frequency *f* could be responsible for the observed instability. However, the possibility that the non-reacting flow conditions (*Re* = 8 x 10^3) lead to the establishment of such structure has to be verified. Data on the evolution of the Strouhal number, defined as $St = \frac{f D_b}{\bar{V}_{inlet}}$, versus the Reynolds number for cylindrical bluff-bodies were first implemented by Relf et al. [21] in a wide range. Then, Roshko [22] extended the study to very high Reynolds numbers. Lienhard [23] gathered the data for this very wide range of Reynolds number (40 to 10^7) to highlight the corresponding regimes. The fully turbulent vortex street regime is proven to be located between Reynolds numbers of 3 x 10^2 and 2 x 10^5. When considering these data, a Reynolds number of 8 x 10^3 seems to fit in a fully turbulent vortex street regime with a Strouhal

number of 0.2. Roshko [24] has experimentally proved the existence of a universal Strouhal number 0.16 ± 0.02 for any bluff-body with any cross-sectional shape.

For reacting-flow conditions, experiments were conducted in the smallest combustion chamber with various bluff-bodies, and a focus was made on flame intensity fluctuations measurements. As shown in Fig. 3, St is a linear function of the diameter and this indicates that vortex shedding is not driving the flame pulsations.

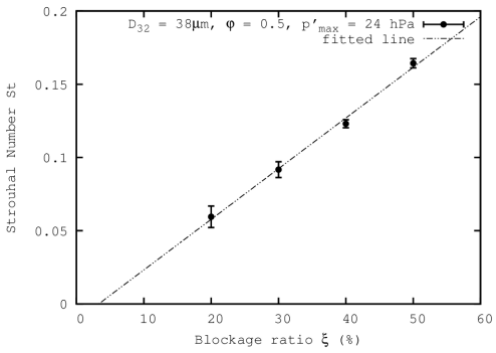

Fig. 3: Strouhal number versus the blockage ratio (%)

As a theoretical proof, it can be reported that Erickson et al. [25] showed that for very high temperature ratio flames ($\frac{T_b}{T_u}$>2), the Von Karman shedding frequency amplitude is reduced to zero and the flame burns in a more centerline-symmetric way. Flames obtained in this study, for the lower equivalence ratio (0.29), presented a minimum temperature ratio of about 3.

b. Pressure and heat release rate fluctuations simultaneous measurements

The relation between pressure and heat release rate is analyzed in this section using synchronized data from both pressure and light intensity sensors. Figure 4 was deduced from some of the data concerning various D_{32} and equivalence ratios, the other parameters being kept constant. Maximum overpressure is stabilized

at about 24 hPa. For every experimental condition studied, the frequency of the pressure fluctuations is identical to the frequency of the light intensity signal.

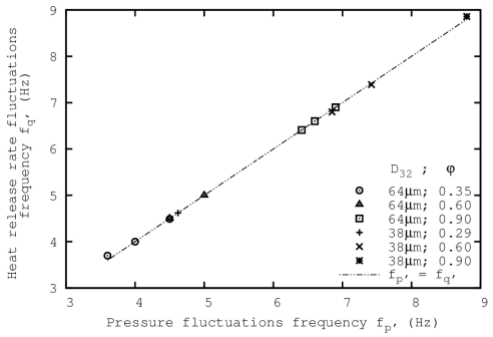

Fig. 4: Heat release rate frequency correlated with pressure fluctuations frequency

The light intensity fluctuations naturally depend on the heat release rate fluctuations. At a first glance, the pressure fluctuations could just be considered as a consequence of velocity fluctuations due to the flame expansion. This induces pressure drop downstream the combustion chamber, where a strong contraction of the flow is located. If this pressure drop was not influencing the flame pulsating behavior, the same frequency would appear whatever the level of pressure drop, since it would only be a consequence of another source of fluctuations. Experiments using different contraction ratios were performed to investigate the influence of the maximum pressure drop on the light intensity fluctuations. Figure 5 gathers the results obtained in the smallest chamber with D_{32} = 38 µm and φ= 0.29, and clearly shows the correlation between those two parameters.

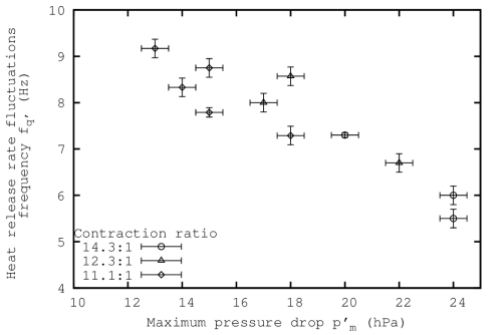

Fig. 5: Heat release rate frequency evolution with maximum pressure drop

The heat release rate frequency decreases in a monotonous way from around 9Hz to around 5Hz by increasing the maximum overpressure from 13 hPa to 24 hPa.

c. Discussion on the feed-back-loop mechanism

A coupling between light intensity and pressure fluctuations has clearly been observed. However, the mechanism behind it is less trivial to establish. A scenario is proposed based on the observations of the combustion frequency f, combustion duration $t_{combustion}$, combustion efficiency η, combustion – pressure delay Δt and their interactions. Combustion duration is obtained by considering the beginning and the end of light emission intensity corresponding respectively to the beginning and the end of the combustion process. Combustion-pressure delay, as depicted in Fig. 2b, is the delay between a peak of heat release rate intensity, i.e. the peak of light intensity, and the following pressure peak.

The most relevant observations for the demonstration are listed hereafter:

1. The combustion frequency increases with the equivalence ratio and decreases with D_{32} (Fig. 4). It decreases also with the pressure drop maximum (Fig. 5) but does not depend on the chamber length.
2. The combustion duration shows a strong concave parabolic tendency with the equivalence ratio with a minimum at φ =0.6. It increases with D_{32} and it is independent of the pressure drop maximum. The combustion durations range from 80 to 160 ms.

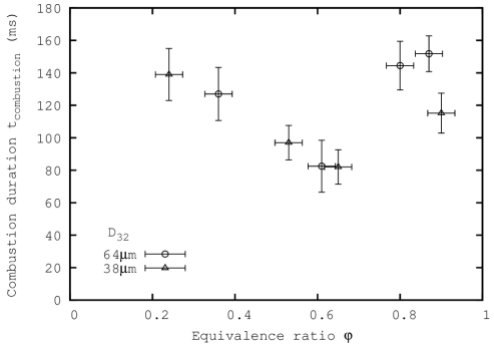

Fig. 6: Combustion duration versus the equivalence ratio

3. The combustion efficiency around the bluff-body has a slight convex parabolic relationship with the equivalence ratio exhibiting a maximum at around φ=0.6. It also decreases with the pressure drop maximum. Local combustion efficiency strongly increases with combustion frequency ranging from 75% to 97%.
4. The combustion-pressure delay slightly decreases with D_{32}. It ranges between 50 to 90 ms.
5. The minimum light emission intensity strongly decreases with pressure drop. It increases with the combustion frequency and equivalence ratio. It varies from 0% to 80% of the maximum light intensity.
6. The global magnesium mass flow rate remains unchanged with overpressure magnitude variations.
7. MgO deposits are observed on the divergent and inlet duct end walls after each experiment.

When removing the diaphragm at the exit duct:

8. At very low overpressure (below 5hPa), the low frequency phenomenon is not observed anymore. Light intensity signals exhibits frequencies two orders of magnitude higher than the former ones.
9. No significant difference is observed on the flame intensity level and on the solid mass flow rate when a steady overpressure, in the range of the maximum overpressures studied, is applied right downstream the Venturi nozzle.

The key factors for the pulsation generation are the extinction and ignition conditions. If the purpose is first to understand why the flame extinguishes, the signals exhibit a declination of light emission occurring exactly when the pressure starts increasing (Fig. 2b).

An aerodynamic interpretation for the flame behavior, supported by the listed observations, is given hereafter. The flame is stabilized in the wake of the bluff-body, which is a zone of low static pressure relatively to the downstream conditions due to strong recirculation. When the sudden increase of pressure drop in the contraction reaches the bluff-body downstream flow through pressure waves, perturbations of the wake may occur and blast the recirculation zone pattern. The duration of this pressure increasing phase is directly related to the maximum pressure drop reached. Indeed, a higher maximum pressure drop means a longer pressure increasing phase (observation 1). Thus, depending on pressure variation magnitude

relatively to the flame holding strength, characterized by equivalence ratio (observations 1 and 5), the flame may partially or completely extinguish. It has been reported by De Champlain [11] that flame holding is at its maximum strength for an equivalence ratio equal to 1, which corresponds to a peak temperature and maximum burning rate conditions.

Another hypothesis, a system instability interpretation, which may be considered for extinction conditions, is the possibility of solid injection perturbations due to an overpressure action on the Venturi part upstream, which may stop the fuel injection until right pressure conditions reappear. However, such interruptions were not noticeable in the magnesium mass flow rate measurements (observation 6) and unburnt magnesium is found in the region of the bluff-body for lower frequencies (observation 3). Observation 9 indicates that a steady overpressure in the combustion chamber does not influence significantly the injection system. Hence, this solid injection perturbation interpretation does not seem to fit well with current observations.

If complete extinction is reached, reignition occurs if pressure reaches a lower limit (Fig. 2.b) with small enough pressure variations so that the recirculation zone can reappear and create conditions of ignition by recirculating hot products and mixture in the wake. The flame then propagates in all directions from the ignition point (Fig. 2.a, observations 2 and 7) generating, with a delay for heat transfer, waves carrying acceleration of gases in the post flame zone. The delay is reduced if the flame propagates faster due to faster heat transfer (observation 4). Increasing the aerosol specific surface area, taken into account by the D_{32}, has a positive effect on flame speed (observation 2). This phenomenon has been observed first, for metals, by Cassel et al. [26], and may explain the decrease of combustion frequency with D_{32} (observation 1) as a longer combustion duration implies longer pressure variation period.

When the diaphragm was removed, even if the low frequency phenomenon was not observed flame fluctuations were still recorded. But the corresponding frequencies were two orders of magnitude higher, which may possibly be related to a transition to acoustically-coupled combustion.

3.2 Effect of the equivalence ratio and combustor length on NO_x production

As already indicated, NO_x emission is an issue for human health and environmental pollution. Combustion engines produce such a pollutant mainly through NO thermal pathway. That is why NO_x emissions are well known for Diesel and gasoline internal combustion engines. After-treatment devices are available for such engines and already implemented in the vehicles. However, reducing NO_x emissions at their source helps avoiding overly complex after-treatment systems and keeping exhaust NO_x emissions below regulated levels. No data have been yet presented on NO_x emission from a metal flame except those of Garra et al. [19]. This section aims to provide a first glance on what could at most be expected with such a combustor. To do so, the equivalence ratio has been varied from 0.29 to 0.98, to observe the evolution of the thermal NO and NO_2 emissions for two size fractions of magnesium powders in different regimes.

For a future power source application development, NO_x emissions must be normalized accounting for the energy produced to give a relevant quantity for benchmarking. The reference points considered are the minimum and maximum NO_x emission of a gasoline commercial engine functioning at about the same chemical power release without any $DeNO_x$ devices. All the combustor data and the maximum emission level of the ICE were normalized again by the minimum emission of the latter, to further simplify the comparison. Figure 7 gives the results versus the equivalent ratio.

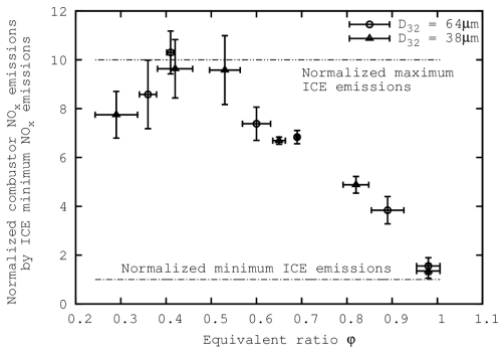

Fig. 7: Normalized NOx emissions versus the equivalence ratio and ICE emissions limits

Before discussion, it must be mentioned that experimental data were verified using a chemical equilibrium software (CEA2 of the NASA Glenn Center) applied to combustion and considering the initial gas and solid composition. A parabolic trend for both experimental and calculated NO_x emissions was obtained as well as an agreement on the maxima positions of NO and NO_2 emissions, respectively around 0.6 and 0.4. Such trends were expected. NO_2 propitious conditions are fuel-lean conditions where lower temperature for its chemical stabilization and enough excess oxygen for NO to NO_2 conversion are present. NO propitious conditions are high enough temperatures so that oxygen is still available in a sufficient amount for the Zeldovich thermal NO pathway [18] to occur.

No significant differences were observed when changing the size range of the powder, which can be characterized by D_{32}, despite of a higher flame temperature for larger magnesium particles [7]. The sensitivity of D_{32} on the flame temperature is not sufficiently important [7] and consequently the NO production by thermal pathway is not really affected by the range of size of magnesium particles.

No significant differences were also observed when changing the combustor length. Such a behavior is surprising as NO production depend on residence time at the right temperature through the kinetic relation :

$$[NO] = \int A e^{-\frac{T_a}{T}} [N_2][O_2]^{0.5} dt \qquad (3)$$

Where A is the pre-exponential factor ($mol^{-0,5}$ s^{-1}), T_a is the activation temperature (K), dt is the residence time (s), species concentrations are between brackets (mol m^{-3}).

The temperature outside the flame zone in the combustor was found to be around 1300 K, at most. It is lower than the minimum temperature required (1700K) for thermal NO production. Hence if the size of the flame remains unchanged for longer combustion chambers, there is no reason for an increase of thermal NO production and emission. The length of the flame was not accurately characterized in this study. However, the measured NO_x level indicates no radical evolution of the flame length.

It can be seen that NO_x emission of the current combustor lies between benchmarked ICE's minimum and maximum emissions. Considering the early phase of development for such a power source, this result is promising. One can consider the implementation of mild combustion [27] using Exhaust Gas Recirculation (EGR) which could be sufficient to reach very low NO_x levels.

4. Conclusion

The study of the magnesium/air combustion fluctuations and NO_x production inside a confined metal combustor by simultaneous pressure, light emission and IR-UV analyzers measurements has revealed some new observations. A coupling between pressure drop variations and heat release rate frequency was identified as the key element in the combustor instability mechanism. Increasing the maximum pressure drop from 13 hPa to 24 hPa, decreases the frequency from 9.2Hz to 5.5Hz. Among the three mechanisms analyzed in this paper, the preferred one suggests that the previous relation is a sign of increased destruction extent of the recirculation zone pattern causing a delay for its reappearance and, by consequence, for the reappearance of reignition conditions. It was observed that equivalence ratio has a positive effect on the combustion frequency. Stronger flame holding or more available heat in the recirculation zone may be the cause of a faster reignition after a partial or a complete extinction, respectively. Normalized NOx emission observations revealed a low level of NO_x: the levels of combustor emissions lie between the two extrema of the ICE current optimized emissions. Further studies will be carried out to tackle all aspects of the combustor needed to achieve such a power source. A deeper characterization of the injection will be performed using high time-resolved mass flow rate measurements to get its sensitivity to the operating conditions. The stability limits of the combustor will be determined to complete the analysis of the aerodynamic interaction with the flame along with thermal characterization of the combustor to estimate the energy cycle efficiency.

Acknowledgments

The authors thank Groupe PSA for the financial support of this study and for all the valuable discussions about scientific and technical aspects.

References

[1] H. M. Cassel, I. Liebman, *Combust. Flame* 6 (1962) 153–156.
[2] G. H. Markstein, *AIAA J.* 1 (3) (1963) 550–562.
[3] S. Gallier, F. Sibe, O. Orlandi, *Proc. Combust. Inst.* 33 (2) (2011) 1949–1956.
[4] J. M. Bergthorson *et al.*, *Appl. Energy* 160 (Supplement C) (2015) 368–382.
[5] J. M. Bergthorson *et al.*, *Appl. Energy* 186, Part 1 (2017) 13–27.
[6] J. Puig, M. Balat-Pichelin, *J. Magnes. Alloys* 4 (2) (2016) 140–150.
[7] R. Lomba *et al.*, *Combust. Sci. Technol.* 188 (11–12) (2016) 1857–1877.
[8] F. Fizaine, *Analyses de la disponibilité économique des métaux rares dans le cadre de la transition énergétique*, PhD thesis, Ecole Doctorale LISIT de Dijon, Dijon, France, 2014.
[9] G. C. Williams, H. L. Hottel, A. C. Scurlock, *Proc. Combust. Inst.* 3 (1949).
[10] J. P. Longwell, *Fourth Symp. Int. Combust.* 4 (1) (1953) 90–97.
[11] J. A. De Champlain, M. F. Bardon, in : Proceedings of the ASME Turbo Expo 1986, Dusseldorf, Germany, 1986.
[12] G. Sotter, J. Swithenbank, *AIAA J.* 2 (7) (1964) 1297–1302.
[13] E. Zukoski, in : *25th AIAA Aerospace Sciences Meeting 1987*, Reno, USA, 1987.
[14] T. Poinsot, *Proc. Combust. Inst.* 36 (1) (2017) 1–28.
[15] J. W. S. Rayleigh, *The Theory of Sound*, Macmillan, London, UK, 1877.
[16] P. J. Langhorne, *J. Fluid Mech.* 193 (1988) 417–443.
[17] P. Degobert, *Automobile et pollution,* Editions Technip, Paris, France, 1992, p. 516.
[18] Y. Zeldovich, D. Frank-Kamenetskii, P. Sadovnikov, *Oxidation of Nitrogen in Combustion,* Publishing House of the Acad of Sciences of USSR, USSR, 1947.
[19] P. Garra *et al.*, *Appl. Energy* 189 (Supplement C) (2017) 578–587.
[20] C. T. Crowe et al., *Multiphase Flows with Droplets and Particles, Second Edition*, CRC Press, Taylor & Francis Group, 2011.
[21] E. F. Relf, L. F. G. Simmons, *Freq. Eddies Gener. Motion Circ. Cylind. Fluid*(917) (1924).
[22] A. Roshko, *J. Fluid Mech.* 10 (3) (1961) 345–356.
[23] J. H. Lienhard, *Synopsis of lift, drag, and vortex frequency data for rigid circular cylinders,* Technical Extension Service, Pullman, USA, 1966.
[24] A. Roshko, *On the drag and shedding frequency of two-dimensional bluff-bodies,* NACA, USA, 1954, p. 16.
[25] R. R. Erickson, M. C. Soteriou, P. G. Mehta, in: *44th AIAA Aerospace Sciences Meeting 2006*, Reno, USA, 2006.
[26] H. M. Cassel, A. K. Das Gupta, S. Guruswamy, *Symp. Combust. Flame Explos. Phenom.* 3 (1) (1948) 185–190.
[27] A. Cavaliere, M. de Joannon, *Prog. Energy Combust. Sci.* 30 (4) (2004) 329–366.

List of figures